Decreasing pH trend estimated from 25-yr time series of carbonate parameters in the western North Pacific

Takashi Midorikawa[1]*, Masao Ishii[1], Shu Saito[1,2], Daisuke Sasano[1], Naohiro Kosugi[1], Tatsuo Motoi[3], Hitomi Kamiya[4], Akira Nakadate[4], Kazuhiro Nemoto[4] and Hisayuki Y. Inoue[5]

[1]Geochemical Research Department, Meteorological Research Institute, Nagamine 1-1, Tsukuba 305-0052, Japan

[2]Institute of Observational Research for Global Change (IORGC), Japan Agency for Marine-Earth Science and Technology (JAMSTEC), Natushima-chou 2-15, Yokosuka 237-0061, Japan.

[3]Oceanographic Research Department, Meteorological Research Institute, Nagamine 1-1, Tsukuba 305-0052, Japan

[4]Global Environment and Marine Department, Japan Meteorological Agency, Otemachi 1-3-4, Chiyoda-ku, Tokyo 100-8122, Japan

[5]Graduate School of Environmental Earth Science, Hokkaido University, N10W5, Kita-ku, Sapporo 060-0810, Japan

*Corresponding author. e-mail: midorika@mri-jma.go.jp

ABSTRACT

We estimated long-term trends of ocean acidification in surface waters in latitudinal zones from 3°N to 33°N along the repeat hydrographic line at 137°E in the western North Pacific Ocean. Estimates were based on the observational records of oceanic CO_2 partial pressure and related surface properties over the last two decades. The computed pH time series both for 25 years in winter (late January to early February) and for 21 years in summer (June to July) exhibited significant decreasing trends in the extensive subtropical to equatorial zones, with interannual variations that were larger in summer. The calculated rates of pH decrease ranged from 0.0015 to 0.0021 yr^{-1} (average, 0.0018 ± 0.0002 yr^{-1}) in winter and from 0.0008 to 0.0019 yr^{-1} (average, 0.0013 ± 0.0005 yr^{-1}) in summer. The thermodynamic effects of rising sea surface temperature (SST) accounted for up to 44% (average, 15%) of the trend of pH decrease in the subtropical region in winter, whereas a trend of decreasing SST slowed the pH decrease in the northern subtropical region (around 25°N) in summer. We used the results from recent trends to evaluate future possible thermodynamic changes in the upper ocean carbonate system.

1. Introduction

The recent uptake of anthropogenic carbon by the ocean has given rise to changes in chemical equilibrium in the surface ocean CO_2 system (Intergovernmental Panel on Climate Change [IPCC], 2007). In particular, the ocean acidification due to the increase in the surface concentrations of CO_2 has recently attracted increasing interest because of possible future positive feedback to global warming resulting from a reduction in the capacity of the ocean to take up additional CO_2 (i.e., to buffer increasing atmospheric CO_2) and because of the potential effects on marine ecosystems.

A decrease in surface pH by 0.1 over the global ocean has been calculated from the estimated uptake of anthropogenic carbon since preindustrial times (Royal Society, 2005), and a further decrease in pH by 0.3–0.4 over the next century is predicted from a model experiment based on estimates of future CO_2 emissions (Caldeira and Wickett, 2003; Orr et al., 2005). To detect such a gradual, long-term ocean acidification requires pH measurements of high precision and traceability. It is only recently that a spectrophotometric method with high precision has been developed (e.g., Clayton and Byrne, 1993), so modern-day changes in surface-water pH have not yet been precisely determined.

The recent time-series data for pH at 25 °C directly measured at the European Station for Time Series in the Ocean at the Canary Islands (ESTOC) in the North Atlantic exhibited a long-term decrease in pH of 0.0017 ± 0.0005 yr^{-1} averaged for 1995–2003 (González-Dávila et al., 2007). Similar trends of decreasing pH at ambient sea surface temperature (SST) were calculated from dissolved inorganic carbon (DIC) and total alkalinity (TA) data at the Hawaii Ocean

Time-series (HOT; Dore et al., 2009; 0.0019 ± 0.0002 yr^{-1}) and the Bermuda Atlantic Time-series Study (BATS; Bates et al., 2007; 0.0017 ± 0.0001 yr^{-1}) sites. However, differences in pH trends between regions or basins over the world oceans are poorly known because of the paucity of long-term time-series observations.

The repeat hydrographic line at 137°E in the western North Pacific, which is a longitudinal section located near the center of the highest sea-surface dynamic height in the subtropical gyre (Fig. 1), is one of the few areas where oceanic CO_2 measurements have been routinely made since the early 1980s. We previously described the latitudinal and seasonal variations of the partial pressure of CO_2 in surface seawater (pCO_2^{sea}) and overlying air (pCO_2^{air}) along 137°E, and the significant increasing trend and interannual variability of winter pCO_2^{sea} (Inoue et al., 1987, 1995; Midorikawa et al., 2005, 2006). The pCO_2^{sea} increased in response to the increase in pCO_2^{air} in all regions studied, from equatorial to subtropical. The increase in pCO_2^{sea} was caused primarily by that in surface DIC due to the oceanic uptake of anthropogenic CO_2, and the relatively small regional differences were attributed mostly to the effects of SST. However, the results indicating unchanged ΔpCO_2 and CO_2 influx over the subtropical region for two decades implied that the northern subtropical region could continue to act as a strong CO_2 sink in the near future. The interannual variations of pCO_2^{sea} from 1983 to 2003 were derived from the different degrees of compensation between the SST and DIC effects on pCO_2^{sea}, which varied with latitude.

In the present study, we specifically focus on the changes in the surface carbonate system producing ocean acidification, on the basis of the long-term pCO_2^{sea} record along 137°E in the

western North Pacific, and discuss the influence of ocean warming on the progress of acidification.

2. Methods

The time series of pH values over the last two decades was estimated based on the observational records of pCO_2^{sea} and related surface properties in the western North Pacific.

2.1. Observation and data

The Japan Meteorological Agency (JMA) and Meteorological Research Institute have been periodically conducting observations of pCO_2^{sea}, pCO_2^{air}, and related hydrographic properties (SST, sea surface salinity [SSS], and others) from south of Japan to the equatorial region along 137°E (Fig. 1) in the western North Pacific during nearly the same periods: from late January to early February since the early 1980s, and in June and July since 1990 (JMA, 2009). The details of the methods have been described by Inoue et al. (1995) and Midorikawa et al. (2006). The data for 1983–2007 used in this study are available from the World Meteorological Organization's World Data Center for Greenhouse Gases (WDCGG; http://gaw.kishou.go.jp/wdcgg.html) operated by JMA.

We have also been conducting precise measurements of DIC, using a coulometric technique and Certified Reference Material provided by Dr. A. G. Dickson at Scripps Institution of Oceanography, at irregular intervals since June 1994 (during the WOCE P9 one-time observations) (Ishii et al., 2001), and pH using a spectrophotometric technique and *m*-cresol purple as an indicator dye since April 2003 (Saito et al., 2008).

2.2. Estimation of total alkalinity

Total alkalinity was not measured, but instead calculated by the methods of Dickson et al. (2007) from SST, SSS, pCO_2^{sea} and DIC for the period after 1994, when these four surface parameters were measured. The calculations used a solubility constant for CO_2 in seawater given by Weiss (1974) and dissociation constants of carbonic acid given by Lueker et al. (2000). The uncertainty of total alkalinity estimates, evaluated from uncertainties of the respective measurements, was less than 4 μmol kg^{-1}. The calculated total alkalinity normalized to a salinity of 35 (n-TA) at the respective latitudes ranged from 2294 ± 4 to 2298 ± 3 μmol kg^{-1} in winter and from 2289 ± 7 to 2296 ± 8 μmol kg^{-1} in summer for the past 14 years, suggesting that n-TA was almost constant (average n-TA of 2295 μmol kg^{-1} at SSS = 35) over the study region and remained unchanged for the study periods, i.e., over the extensive regions from 3–33°N, the calculated n-TA showed little variability in either space or time over the past 14 years (Fig. 2).

2.3. Estimation of pH

The time series of pH values were calculated for the period of 1983–1993 by the methods of Dickson et al. (2007) using the time series data for pCO_2^{sea}, SST and SSS, and assuming TA of 2295/35* SSS μmol kg^{-1}. For total alkalinity, a constant n-TA of 2295 μmol kg^{-1} at S = 35, the average value over the most recent 14 years, was converted to the TA value at a ambient SSS, proportional to the salinity. For this study, pH values were expressed on the pH scale of total

hydrogen ion concentration (Dickson et al., 2007).

For 2003–2008, when pH was measured along with SST, SSS, and surface pCO_2^{sea} and DIC, surface pH values calculated from these four parameters were compared with measured ones (Fig. 3). The calculated and measured pH values for 2003–2008 were in good agreement; the differences averaged 0.0026 ± 0.0050 (mean ± 1σ) in winter and 0.0003 ± 0.0052 in summer, supporting the validity of the calculation procedures.

2.4. Normalization of pH and pCO_2^{sea}

Normalization of pH to a constant SST of 25 °C was also based on the computation routine of carbonate equilibrium using the methods of Dickson et al. (2007). In this study, because total alkalinity throughout the entire period was assumed, time series of DIC were also able to be calculated. Then, pH at a constant SST of 25 °C (pH_{T25}) was calculated from time series of observed pCO_2^{sea} and SSS as well as calculated DIC.

Normalization of pCO_2^{sea} to constant values of SST and SSS was usually calculated by using the empirical equation (e.g., Weiss et al., 1982). In this study, however, because time series of DIC were estimated, as mentioned above, pCO_2^{sea} at the mean SST and SSS (n-pCO_2^{sea}) was calculated from time series of observed pCO_2^{sea} and calculated DIC, using the methods of Dickson et al. (2007). The calculated n-pCO_2^{sea} values were in good agreement with those calculated empirically according to the equations by Midorikawa et al. (2006), derived from the integration of the equation by Weiss et al. (1982); the differences between two calculation were 0.02 ± 0.33 µatm, which was

smaller than the overall precision of pCO_2^{sea} measurements (<3 µatm) (Midorikawa et al., 2006).

3. Results and Discussion

3.1. Long-term changes in pCO_2^{air} and pCO_2^{sea}

The time-series data for pCO_2^{air} showed similar, linearly increasing trends with little interannual variability at all latitudes along 137°E in both winter and summer, whereas pCO_2^{sea} showed substantial increasing trends with a larger interannual variability over the entire area, from the subtropical to equatorial regions, in both winter and summer (Figs. 4a and c). The values for pCO_2^{sea} were lower than pCO_2^{air} in winter because of lower SST at higher latitudes, whereas, in summer, pCO_2^{sea} values were higher than pCO_2^{air} because of the effects of high SST exceeding those of lowering DIC. The magnitude of pCO_2^{sea} interannual variability was relatively large at latitudes south of 20°N in winter and north of 24°N in summer. Furthermore, the interannual variability of pCO_2^{sea} in summer was larger than that in winter, especially owing to larger SST variability from 25°N to 31°N.

3.2. Long-term changes in pH at ambient SST

The estimated pH (Fig. 5a) was higher at high latitudes than at low latitudes in winter because of a large latitudinal gradient of SST (Fig. 4b). By contrast, pH normalized to a constant SST of 25 °C, pH_{T25}, was lower at high latitudes than at low latitudes because of higher DIC concentrations

at higher latitudes (Ishii et al., 2001). In summer, the latitudinal differences in pH disappeared because of a much smaller north–south SST gradient. The time-series pH data in both winter and summer at all latitudes exhibited distinct long-term decreasing trends with notable interannual variation but without readily recognizable periodicity. The interannual variability of pH was also large in summer.

We calculated the average rate of pH decrease for each 1° of latitude along 137°E for the entire study period using the linear least-squares method. The rates of decrease ranged from (mean ± 1 standard deviation [1σ]) 0.0015 ± 0.0002 to 0.0021 ± 0.0002 yr^{-1} (average, 0.0018 ± 0.0002 yr^{-1}) in winter (Fig. 6e) and from 0.0008 ± 0.0004 to 0.0019 ± 0.0005 yr^{-1} (average, 0.0013 ± 0.0005 yr^{-1}) in summer (Fig. 7e). These trends were significant at most latitudes south of 33°N: $p <$ 0.001 at all latitudes in winter; $p < 0.05$ at 26 latitudes and $0.05 < p < 0.1$ at five latitudes in summer. The range of these decreasing pH rates in the present study area (3–33°N) was comparable to that (0.0017 ± 0.0005 yr^{-1}) directly measured at 25 °C at ESTOC (29°10'N) in the North Atlantic (González-Dávila et al., 2007) and those calculated at ambient SST for the HOT (22°45'N; 0.0019 ± 0.0002 yr^{-1}; Dore et al., 2009) and BATS sites (31°50'N; 0.0017 ± 0.0001 yr^{-1}; Bates et al., 2007). These similar trends in different regions of the ocean could reflect the rapid response of pCO_2^{sea} to changes in pCO_2^{air}, and furthermore, suggest no intrinsic difference in the changes in the surface carbonate system between these subtropical regions.

3.3. Contribution of changes in SST to those in pH and DIC

The rates of decreasing pH_{T25} were similar in winter (average, 0.0015 ± 0.0003 yr^{-1}) and summer (average, 0.0014 ± 0.0004 yr^{-1}). The steeper decreasing trends of pH at ambient SST in winter were attributed to the effects of a relatively greater rate of SST increase in winter (range, –0.03 to 0.06 °C yr^{-1}; average, 0.02 ± 0.02 °C yr^{-1}; Fig. 6a), compared with those in summer (–0.07 to 0.04 °C yr^{-1}; average, –0.01 ± 0.02 °C yr^{-1}; Fig. 7a), although these SST trends were insignificant. These results are consistent with similar trends in the calculated n-DIC (DIC normalized to a salinity of 35) in winter (range, 0.6 to 1.4 µmol kg^{-1} yr^{-1}; average, 0.96 ± 0.16 µmol kg^{-1} yr^{-1}; Fig. 6d) and summer (0.5 to 1.5 µmol kg^{-1} yr^{-1}; average, 0.92 ± 0.26 µmol kg^{-1} yr^{-1}; Fig. 7d).

The rate of increase in pCO_2^{sea} (average, 1.58 ± 0.12 µatm yr^{-1} in winter and 1.37 ± 0.33 µatm yr^{-1} in summer; Figs. 6c and 7c) was not significantly different from that of pCO_2^{air} (average, 1.65 ± 0.05 µatm yr^{-1} in winter and 1.54 ± 0.08 µatm yr^{-1} in summer). However, the time series pCO_2^{sea} data in each latitude range normalized to the mean temperature and salinity for the entire period, n-pCO_2^{sea}, exhibited a pattern of lower rates of n-pCO_2^{sea} increase in latitudes showing increasing trends in SST, and higher rates in latitudes with decreasing SST trends, yielding a latitudinal distribution with relatively lower rates of increase in the southern region of the study area (especially, Fig. 7c).

These characteristics were the same in the trends of n-DIC and pH_{T25} (Figs. 6 and 7) calculated on the assumption of a constant n-TA. These results suggest that the long-term response of the surface carbonate system to the anthropogenic CO_2 increase in the atmosphere could be

predominantly through increases in pCO_2^{sea}, in response to the changes in pCO_2^{air}. Therefore, in latitudes with increasing SST trends, larger temperature effects could allow pCO_2^{sea} to keep up with the pCO_2^{air} level even in areas with a smaller rate of n-DIC increase, and consequently, further depress the n-DIC increase rate; decreasing SST trends would conversely induce higher rates of DIC increase.

These temperature effects could also extend to the magnitude of pH rate of decrease; in latitudes with increasing SST trends, a smaller rate of n-DIC increase would produce a more gradual decreasing pH_{T25} trend. For pH at ambient SST, larger effects of increasing SST trends, acting to decrease pH, could make up for those of the lower rates of n-DIC increase, leading to significant decreasing pH trends.

For the individual rate at each latitude, the effects of changing SST accounted for –25% to 44% (average, 15%) in winter and –85% to 37% (average, –10%) in summer of the decreasing pH trends (Figs. 6e and 7e). Compared with the rates of pH_{T25}, the trend of increasing SST elevated the decreasing trend in pH at ambient SST in most latitudes (27 latitudes) in winter and the decreasing SST reduced the rates of decreasing pH at ambient SST in the northern subtropical region (a maximum of 46% against pH_{T25} at 25°N) in summer.

Conspicuously low rates of change in pH_{T25} were found around 23–24°N in winter, together those of n-pCO_2^{sea} and n-DIC, corresponding to high rates of SST increase (Figs. 6 and 7). Midorikawa et al. (2006) indicated that the close coupling of interannual variations between the surface DIC concentrations and SST in these latitudes could be attributed to the influence of the

interannual north–south movement of the Subtropical Front, which forms the boundary between the northern cold, DIC-rich water mass and the southern warm, DIC-poor water mass (Ishii et al., 2001), in addition to inverse DIC–SST anomaly relationships derived from winter vertical mixing. The position of the Subtropical Front, denoted by a surface potential density σ_θ of 24 (or SST of 22 °C) in winter, exhibited a long-term tendency to shift to the north: 0.5 ± 0.3 degrees of latitude per decade during 1983–2007 (p = 0.10) and 0.29 ± 0.15 deg per decade during 1967–2007 (p = 0.07), based on hydrographic observations (JMA, 2001, 2008), and 0.22 ± 0.09 deg per decade during 1951–2007 (p = 0.01) based on SST reanalysis (Ishii et al., 2005). The long-term northward shift of the Subtropical Front could lead to the trends described earlier for the carbonate system properties and SST in these latitudes.

3.4. Long-term changes in pH since 1969

Paired data for SST, SSS, TA, and pCO_2^{sea} was acquired at five latitudes from 9°N to 30°N around 158°E in February 1970 (Inoue et al., 1999). The n-TA values ranged in 2297 ± 3 μmol kg^{-1}, which is similar to those estimated for 1994–2007 (Fig. 2). Considering the effects of SST variations, the pH_{T25} values from these 1970 data were lower by 0.002 ± 0.006 to 0.030 ± 0.009 than those estimated for 1970 from the extrapolation of the pH_{T25} trends in the same latitudes for the past 25 years in the present study. The rate of pH_{T25} decrease for 1970–1983 was calculated as 0.0009 ± 0.0006 yr^{-1}, which is smaller than those for the more recent trends. The difference between SST observed in 1970 and the average at the same latitude for 1983–2007 was 0.12 ±

0.82 °C, which was smaller than 1σ value (0.66 °C, the average in the entire area) for the interannual variability of SST during the past 25 years, indicating that 1970 was not an anomalous year. Moreover, data set of SST, SSS, and pCO_2^{sea} at latitudes from 3°N to 30°N around 138°E in February 1969 (the average anomaly, -0.17 ± 0.60 °C for 1969; Inoue et al., 1999) also gave a low average rate of pH_{T25} decrease (0.0008 ± 0.0006 yr^{-1},) for 1969–1983, assuming TA of 2295/35* SSS μmol kg^{-1}. Although a determination of acidification based on snapshot observations from two specific years is difficult because interannual variations must also be considered, these data suggest an acceleration of acidification after the 1980s.

3.5. Estimation of changes in pH during the next 50 years

The observational records of pCO_2^{sea} and the time series of pH estimated on the basis of these data in the western North Pacific for the past 25 years were in agreement with long-term trends calculated from the atmospheric CO_2 increase. We therefore estimated the future trends of ocean acidification in the western subtropical North Pacific Ocean on the assumption that only the changes derived from the atmospheric CO_2 increase could continue to dominate changes in the surface carbonate system in these regions without altering the ecosystems and other factors related to the carbon cycle, excluding SST. Thus, the magnitude of future ocean acidification attributable to thermodynamic changes in the surface carbonate system of the western subtropical North Pacific over the next 50 years was tentatively evaluated for the following two cases. Case 1 used the same rate of pCO_2^{sea} increase as that observed for the past 25 years, i.e., the extrapolation of the recent

trend of pCO_2^{sea} increase. Case 2 assumed a rapid response of pCO_2^{sea} to the pCO_2^{air} changes predicted in accordance with future CO_2 emission scenario IS92a in IPCC (2007).

Calculations were performed using the results of winter observations averaged in two representative realms: the northern (25–28°N) and southern (11–14°N) subtropical regions. The northern region is located near the center of the highest sea surface dynamic height in the western subtropical gyre, and the southern region is located in the southern half of the North Equatorial Current (Fig. 1). For the past 25 years, SST showed an insignificant trend (0.009 ± 0.018 °C yr^{-1}, p = 0.6) in the northern region, whereas a trend of increasing SST (0.020 ± 0.013 °C yr^{-1}, p = 0.12) was observed in the southern region, although this trend was not statistically significant. For Case 1, two sets of calculations, with and without SST changes, were compared (Table 1).

In Case 1, the magnitudes of n-DIC and pH changes from calculations ignoring SST increases were 45 to 50 μmol kg^{-1} for n-DIC and –0.073 to –0.085 for pH, respectively, over the next 50 years (Table 1, Fig. 8). Under a constant SST, the rates of n-DIC increase in the two regions for 2040–2060 were 14–24% lower, and the rates of pH decrease were 21–22% lower, than the rates for 1983–2007. We attribute this decrease in the rates of change to the increase in the buffer factor (Revelle and Suess, 1957) from the increase in DIC.

When the same trend of increasing SST for the past 25 years is assumed for the future, the rates of n-DIC increase are reduced an additional 5–18%, whereas there is almost no change to the projected rates of pH decrease in either region for 2040–2060 (a reduction of <1% to 1%). Under these conditions, the effects of increasing SST compensated for the slowing of the rate of pH

decrease resulting from the reduction in the rate of DIC increase from the increase in the buffer factor.

In Case 2, under the future CO_2 emission scenario IS92a, larger amounts of oceanic CO_2 uptake were predicted considering the past SST trend, leading to an additional n-DIC increase of 24 μmol kg^{-1} and subsequent additional pH decrease of 0.04 (total pH decrease of 0.11 to 0.13 over the next 50 years; Table 1, Fig. 9), compared with Case 1. The rates of both n-DIC increase and pH decrease for 2040–2060 were notably higher in the two regions, compared with those for the past 25 years and those in Case 1. The predicted rates of pH decrease for 2040–2060 were about 40% greater than those from recent years. It is therefore possible that future ocean acidification could be accelerated, depending on increases in CO_2 emissions. The magnitudes of the total pH decreases estimated in the present study are less than that predicted for the average over the global ocean in previous reports (a decrease of approximately 0.2 by the year 2050) (Caldeira and Wickett, 2003; Orr et al., 2005).

Our calculations in the present study are confined within the equilibria among the dissolved and ionic carbonate species, as mentioned in the section of Methods. Recent studies have indicated possible future changes in marine ecosystems resulting from global warming, ocean acidification, or both. Recent reports on the effects of ocean acidification on the structure and function of marine microbial communities under high CO_2 conditions (e.g., Doney et al., 2009) suggest significant feedbacks to the upper ocean carbon cycle through related biogeochemical processes. It is important to monitor the surface carbonate system through time-series observations, including high-precision

pH measurements as well as the information on the formation of $CaCO_3$ and organic matter, to determine the future trends of acidification in the upper water column, and to detect changes in the surface carbonate system. Future studies using time-series data over extensive regions are required to determine the effects of changes in marine ecosystems on the upper-ocean carbon cycle.

4. Conclusions

We firmly evaluated the trend of ocean acidification in surface layer of the western North Pacific using the data of partial pressure of CO_2 acquired for the period 1983-2007 when no precise data of pH was available. Time series of pH estimated at ambient SST exhibited distinct long-term trend of acidification (~0.01 to 0.02 pH unit per decade) over the regions from the tropical to the northern subtropical zone in both winter and summer. The magnitude of pH decrease in these regions was close to those reported for other subtropical regions (HOT, BATS and ESTOC sites). These similar trends in different regions of the ocean suggest that the long-term response of the surface carbonate system to the anthropogenic CO_2 increase in the atmosphere could be predominantly through increases in only pCO_2^{sw} (but not DIC), in response to the changes in pCO_2^{air}.

The comparisons of the pH decreasing rate for the past 25 years with those for a decade since 1969 and for the next 50 years suggest an acceleration of the acidification in recent years, as well as in the future depending the scenario. Our analysis exhibited that, in latitudes with increasing SST trends, its larger thermodynamic effects to decrease pH at ambient SST exceeded those to

depress n-DIC increase, leading to larger decreasing pH trends. These results suggest that the future ocean warming could also be a factor accelerating the acidification through its thermodynamic effects. Continual monitoring of the qualitative and quantitative changes in the surface carbonate system through time-series observations, including high-precision pH measurements, is required in future study.

Acknowledgments

The authors are grateful to the past and present staff of the Marine Division (and former Oceanographical Division), Global Environment and Marine Department, Japan Meteorological Agency, for their efforts in maintaining the monitoring program, and to the captains and crew of the of R/V *Ryofu Maru* and *Keifu Maru* for their kind cooperation in the measurements and collection of samples during the cruises in 1983–2007. We also thank editor and an anonymous reviewer for their helpful comments. Finally, we acknowledge the staff of the Geochemical Research Department of the Meteorological Research Institute for their support of this work. This research was partly supported by the “Global Environment Research Fund by the Ministry of the Environment Japan” D-0803.

References

Bates, N. R., 2007. Interannual variability of the oceanic CO_2 sink in the subtropical gyre of the North Atlantic Ocean over the last 2 decades. *J. Geophys. Res*., **112**, C09013, doi:10.1029/2006JC003759.

Dore, J. E., Lukas, R., Sadler, D.W., Church, M. J. and Karl, D. M., 2009. Physical and biogeochemical modulation of ocean acidification in the central North Pacific. *Proc. Nat. Acad. Sci*., **106**, 12235-12240.

Caldeira, K. and Wickett, M. E. 2003. Anthropogenic carbon and ocean pH. *Nature*, **425**, 365.

Clayton, T. D. and Byrne, R. H. 1993. Spectrophotometric seawater pH measurements: total hydrogen ion concentration scale calibration of *m*-cresol purple and at-sea results. *Deep-Sea Res. I*, **40**, 2115-2129.

Dickson, A. G., Sabine, C. L. and Christian, J. R. (Eds.) 2007. *Guide to best practices for ocean CO_2 measurements*. PICES Special Publication 3, 191 pp.

Doney, S. C., Fabry, V. J., Feely, R. A. and Kleypas, J. A. 2009. Ocean acidification: The other CO_2 problem. *Annu. Rev. Mar. Sci*., **1**, 169−192, doi:10.1146/annurev.marine.010908.163834.

González-Dávila, M., Santana-Casiano, J. M. and González-Dávila, E. F. 2007. Interannual variability of the upper ocean carbon cycle in the northeast Atlantic Ocean. *Geophys. Res. Lett*., **34**, L07608, doi:10.1029/2006GL028145.

Inoue, H., Sugimura, Y. and Fushimi, K. 1987. pCO_2 and $\delta^{13}C$ in the air and surface sea water in the western North Pacific. *Tellus*, **39B**, 228-242.

Inoue, H. Y., Matsueda, H., Ishii, M., Fushimi, K., Hirota, M., Asanuma, I. and Takasugi, Y. 1995. Long-term trend of the partial pressure of carbon dioxide (pCO_2) in surface waters of the western North Pacific, 1984-1993. *Tellus*, **47B**, 391-413.

Inoue, H. Y., Ishii, M., Matsueda, H., Saito, S., Midorikawa, T. and Nemoto, K. 1999. MRI measurements of partial pressure of CO_2 in surface waters of the Pacific during 1968 to 1970: re-evaluation and comparison of data with those of the 1980s and 1990s. *Tellus*, **51B**, 830-848.

Intergovernmental Panel on Climate Change (IPCC) 2007. *Climate Change 2007: The Physical Science Basis*. Contribution of Working Group I to the Fourth Assessment Report of the Intergovernmental Panel on Climate Change, Cambridge University Press, Cambridge, UK and New York, NY, USA, 996 pp.

Ishii, M., Inoue, H. Y., Matsueda, H., Saito, S., Fushimi, K., Nemoto, K., Yano, T., Nagai, H. and Midorikawa, T. 2001. Seasonal variation in total inorganic carbon and its controlling processes in surface waters of the western North Pacific subtropical gyre. *Mar. Chem.*, **75**, 17-32.

Ishii, M., Shouji, A., Sugimoto, S. and Matsumoto, T. 2005. Objective analyses of sea-surface temperature and marine meteorological variables for the 20th Century using ICOADS and the Kobe Collection. *Int. J. Climatol.*, **25**, 865-879.

Japan Meteorological Agency (JMA) 2001. *Data Report of Oceanographic Observations, Special Issue, No. 1 (Data: 1965-1992)* [CD-ROM], Tokyo.

Japan Meteorological Agency (JMA) 2008. *Data Report of Oceanographic and Marine*

Meteorological Observations, No 97 (Data: 1993-2006) [CD-ROM], Tokyo.

Japan Meteorological Agency (JMA) 2009. *Annual Report on Atmospheric and Marine Environment Monitoring No. 9, Observation Results for 2007* [CD-ROM], Tokyo.

Lueker, T. J., Dickson, A. G. and Keeling, C. D. 2000. Ocean pCO_2 calculated from dissolved inorganic carbon, alkalinity, and equations for K_1 and K_2: validation based on laboratory measurements of CO_2 in gas and seawater at equilibrium. *Mar. Chem.*, **70**, 105-119.

Midorikawa, T., Nemoto, K., Kamiya, H., Ishii, M. and Inoue, H. Y. 2005. Persistently strong oceanic CO_2 sink in the western subtropical North Pacific. *Geophys. Res. Lett.*, **32**, L05612, doi:10.1029/2004GL021952.

Midorikawa, T., Ishii, M., Nemoto, K., Kamiya, H., Nakadate, A., Masuda, S., Matsueda, H., Nakano, T. and Inoue, H. Y. 2006. Interannual variability of winter oceanic CO_2 and air-sea CO_2 flux in the western North Pacific for 2 decades. *J. Geophys. Res.*, **111**, C07S02, doi:10.1029/2005JC003095.

Orr, J. C., Fabry, V. J., Aumont, O., Bopp, L., Doney, S. C., and co-authors. 2005. Anthropogenic ocean acidification over the twenty-first century and its impact on calcifying organisms. *Nature*, **437**, 681-686.

Revelle, R. and Suess, H. E. 1957. Carbon dioxide exchange between atmosphere and ocean and the question of an increase of atmospheric CO_2 during the past decades. *Tellus*, **9**, 18-27.

Royal Society 2005. Ocean acidification due to increasing atmospheric carbon dioxide. Policy Document 12/05, The Royal Society, London, 223 pp.

Saito, S., Ishii, M., Midorikawa, T. and Inoue, H. Y. 2008. Precise spectrophotometric measurement of seawater pH_T with an automated apparatus using a flow cell in a closed circuit. *Technical Reports of the Meteorological Research Institute*, **57**, Tsukuba, 28 pp.

Weiss, R. F. 1974. Carbon dioxide in water and seawater: the solubility of a non-ideal gas. *Mar. Chem.*, **2**, 203–215.

Weiss, R. F., Jahnke, R. A. and Keeling, C. D. 1982. Seasonal effects of temperature and salinity on the partial pressure of CO_2 in seawater. *Nature*, **300**, 511-513.

Figure captions

Fig. 1. Locations of the repeat observation line (black bold line) and major currents along 137°E in the western North Pacific. Color shade represents the sea-surface dynamic height averaged for 2000 to 2004.

Fig. 2. Time series of n-TA (total alkalinity normalized to a salinity of 35) calculated from observed SST, SSS, pCO_2^{sea}, and DIC in latitudes 3–33°N along 137°E in winter (closed circles) and summer (open diamonds) for the period after 1994. Broken line denotes the average n-TA value of 2295 μmol kg^{-1} for the study periods.

Fig. 3. Comparison between calculated and observed pH values for the most recent 5 yr (2003–2008). Blue, winter data; red, summer. Error bars represent uncertainties for the respective pH values. The uncertainties are 0.002 for observed pH values from the pH measurements (Saito et al., 2008) and 0.003 for calculated values from the measurements of pCO_2^{sea} (<2 μatm) and DIC (<2 μmol kg^{-1}).

Fig. 4. Time series of pCO_2^{air}, pCO_2^{sea} and SST at six latitudes along 137°E. (a) pCO_2^{sea} and (b) SST in winter; and (c) pCO_2^{sea} and (d) SST in summer. Red circles, 3°N; violet triangles, 10°N; orange diamonds, 15°N; green squares, 20°N; light blue triangles, 25°N; and blue circles, 30°N. In (a) and (c), time series of pCO_2^{air} are also shown by dotted lines ranging from black (30°N) to pale gray (3°N).

Fig. 5. Time series of surface-water pH estimated for ambient SST at six latitudes along 137°E in

winter (a) and summer (b). Symbols are defined as in Fig. 4.

Fig. 6. Latitudinal distributions of long-term trends for (a) SST, (b) salinity, (c) pCO_2^{sea}, (d) n-DIC, (e) pH, and (f) buffer factor in winter. In (c), pCO_2^{sea} (blue circles) is presented along with n-pCO_2^{sea} (pCO_2^{sea} normalized to average temperature and salinity; red squares) and pCO_2^{air} (open squares). In (e), pH estimates are presented for ambient SST (blue circles) and normalized to 25 °C (pH_{T25}; red squares). Error bars represent 1σ values for the rates of change at each latitude. In (f), buffer factor ($\partial \ln pCO_2^{sea} / \partial \ln DIC$) was calculated at observed SST and SSS and calculated TA (from constant n-TA).

Fig. 7. Same as Fig. 6, but for summer.

Fig. 8. Estimated trends for the next 50 years for Case 1. Trends based on the extrapolation of rates of increase for pCO_2^{sea} in winter (closed circles), averaged in the northern (25–28°N, blue) and southern (11–14°N, red) regions along 137°E over the past 25 years, were compared with trends based on the extrapolation of the trends over the past 25 years (dotted line 1). (a) pCO_2^{sea}, (b) n-DIC, (c) pH, (d) buffer factor. Future trends were estimated ignoring (broken line 2) and including SST changes (bold line 3). In (d), buffer factor ($\partial \ln pCO_2^{sea} / \partial \ln DIC$) was calculated at constant SST (average values for 1983–2007) for broken line 2 and at SST with the same trends as those observed for the past 25 years for bold line 3 as well as constant SSS and TA (average values for 1983–2007).

Fig. 9. Comparison of future trends between Case 1 (extrapolation of past pCO_2^{sea} trend; broken line C1) and Case 2 (CO_2 emission scenario IS92a [IPCC, 2007]; bold line C2) with consideration

of past SST change in the northern (25–28°N, blue) and southern (11–14°N, red) regions. (a) pCO_2^{sea}, (b) n-DIC, (c) pH, and (d) buffer factor. Dotted line denotes the extrapolations of recent trends. In (d), buffer factor ($\partial \ln pCO_2^{sea} / \partial \ln DIC$) was calculated at SST with the same trends as those observed for the past 25 years as well as constant SSS and TA (average values for 1983–2007).

Table 1. Estimates of thermodynamic changes in the surface carbonate system over the next 50 years for Case 1 (extrapolation of recent rates of pCO_2^{sea} increase) and Case 2 (CO_2 emission scenario IS92a in IPCC [2007]).

Estimation period	n-DIC change			pH change			Buffer factor[c]
	Magnitude[a] (μmol kg^{-1})	Rate (μmol kg^{-1} yr^{-1})	Ratio[b] (%)	Magnitude[a]	Rate (yr^{-1})	Ratio[b] (%)	
1983–2007							
11–14°N	23 ± 3	0.92 ± 0.10		–0.042 ± 0.003	–0.0017 ± 0.0001		8.8 ± 0.2
25–28°N	28 ± 4	1.12 ± 0.14		–0.049 ± 0.004	–0.0020 ± 0.0002		9.3 ± 0.1
Case 1 for 2040–2060							
11–14°N without SST trend	45 ± 6	0.79 ± 0.34	86	–0.073 ± 0.010	–0.0013 ± 0.0006	79	9.5 ± 0.3
with SST trend	36 ± 11	0.63 ± 0.51	68	–0.074 ± 0.010	–0.0013 ± 0.0006	79	9.3 ± 0.6
25–28°N without SST trend	50 ± 4	0.85 ± 0.26	76	–0.085 ± 0.008	–0.0015 ± 0.0005	78	10.1 ± 0.2
with SST trend	46 ± 11	0.79 ± 0.55	71	–0.085 ± 0.008	–0.0015 ± 0.0005	79	10.0 ± 0.7
Case 2 (with SST trend) for 2040–2060							
11–14°N	60 ± 10	1.24 ± 0.48		–0.114 ± 0.010	–0.0024 ± 0.0006		9.8 ± 0.6
25–28°N	70 ± 11	1.40 ± 0.52		–0.129 ± 0.008	–0.0027 ± 0.0005		10.5 ± 0.7

[a]For Cases 1 and 2, the magnitude is the estimated change from 2000 to 2050.

[b]Ratio between the estimated rate for Case 1 to the observed rate for 1983–2007, expressed as a percentage.

[c]Buffer factor ($\partial \ln pCO_2^{sea} / \partial \ln DIC$): values calculated at observed SST and SSS and calculated TA for 2000 from observation data for 1983–2007; estimates at constant SSS and TA (average values for 1983–2007) for 2050 for Cases 1 and 2 (SST trends are from observation data for 1983–2007).

Fig. 1

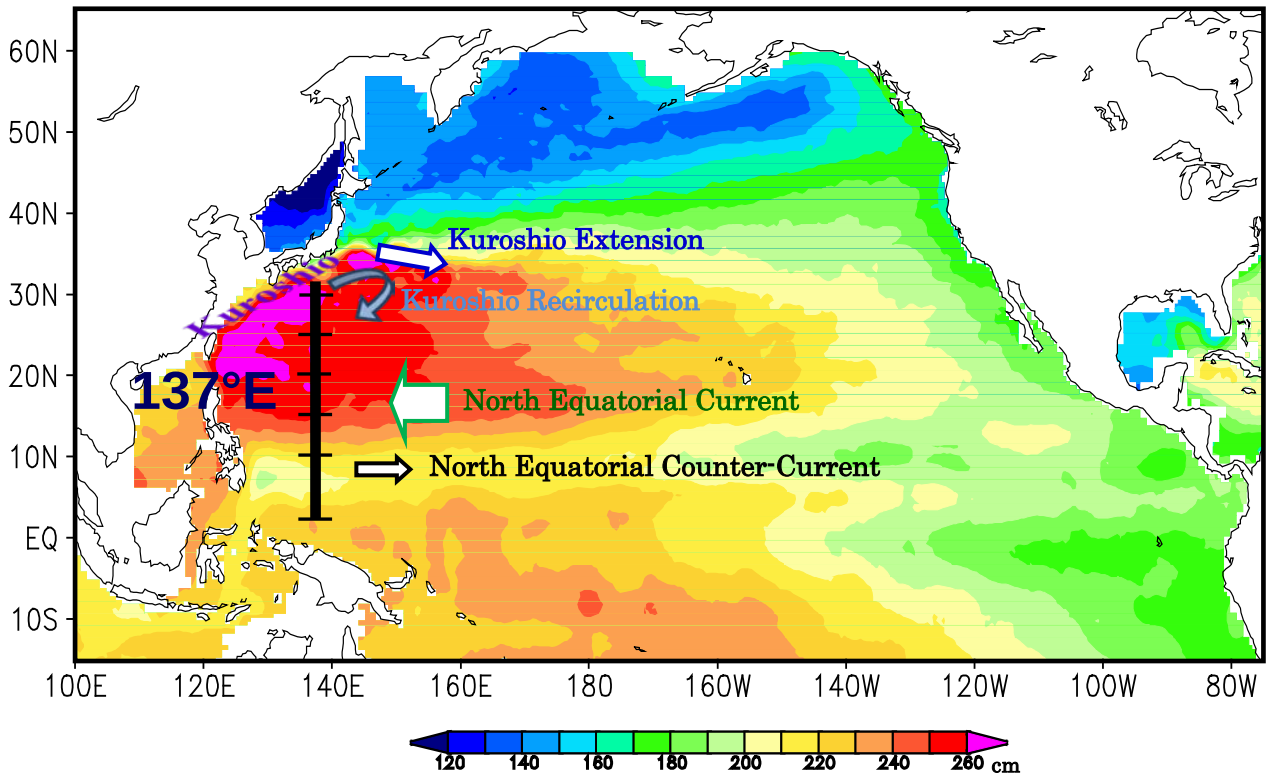

Sea Surface Dynamic Height (average 2000–2004)

Fig. 2

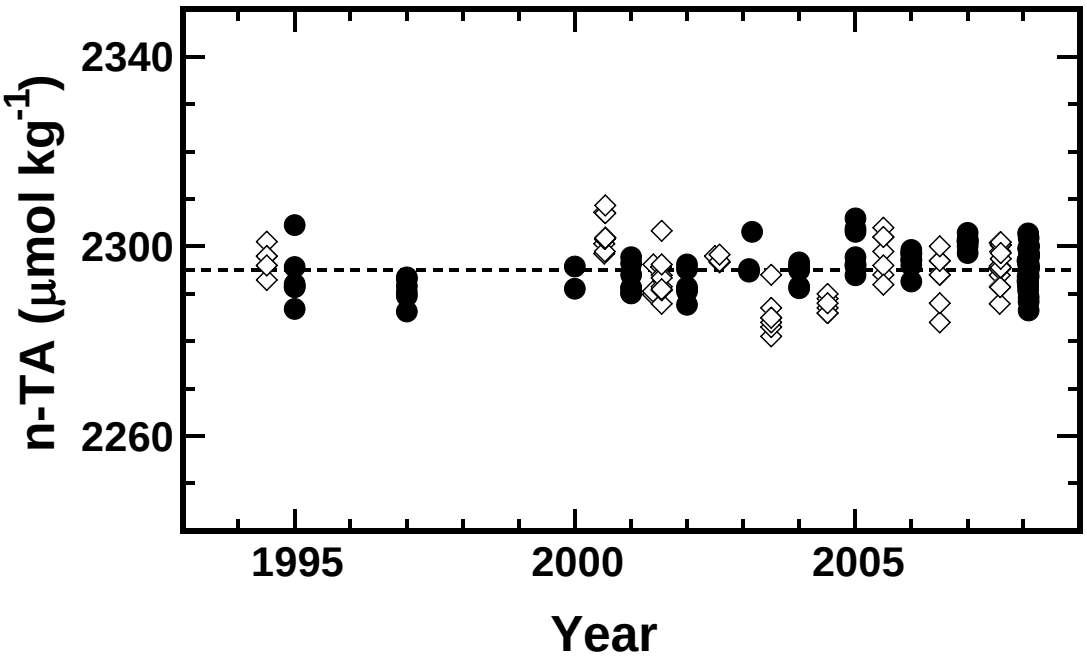
2340
2300
2260
n-TA (µmol kg-1)
1995
2000
2005
Year

Fig. 3

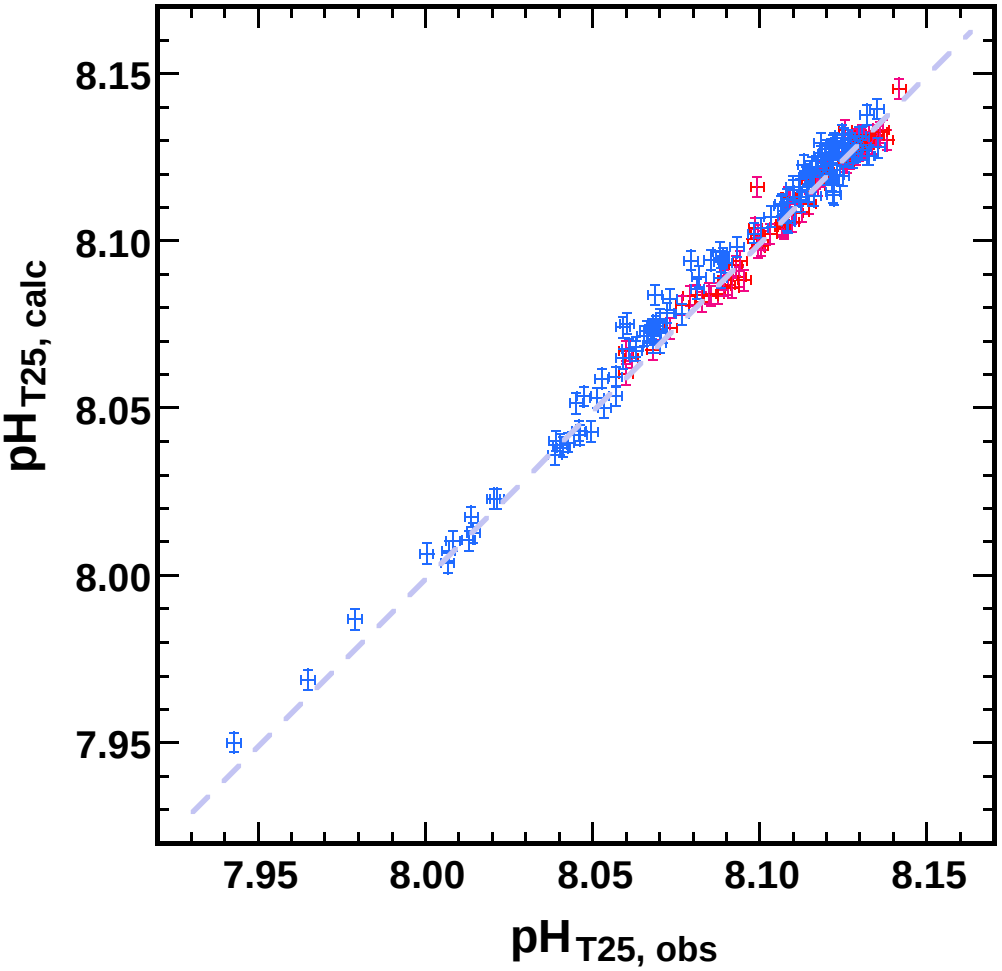
8.15
8.10
8.05
8.00
7.95
pHT25, calc
7.95
8.00
8.05
8.10
8.15
pHT25, obs

Fig. 4

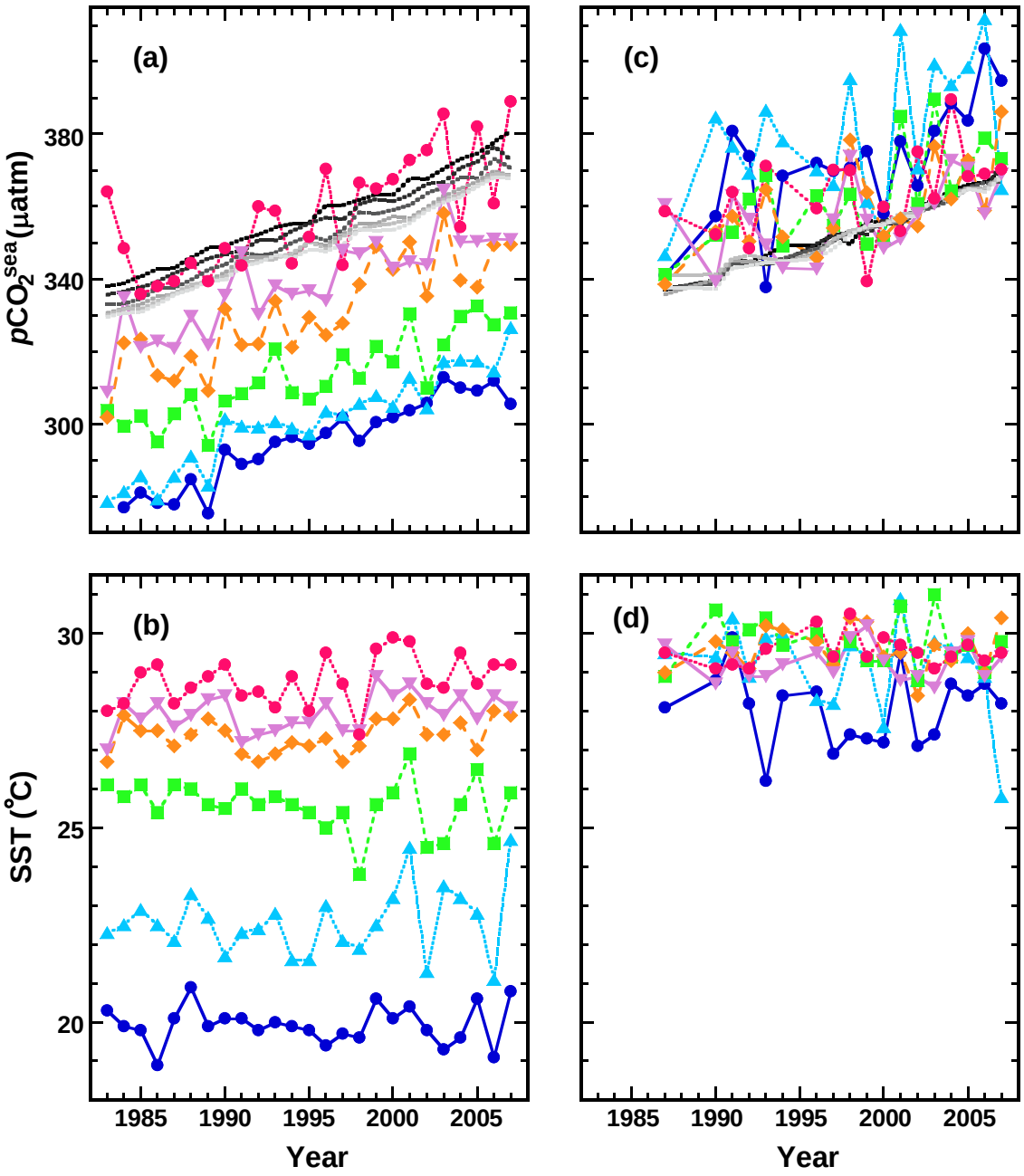
(a)
(c)
(b)
(d)
pCO_2^{sea} (µatm)
380
340
300
SST (°C)
30
25
20
1985
1990
1995
2000
2005
Year

Fig. 5

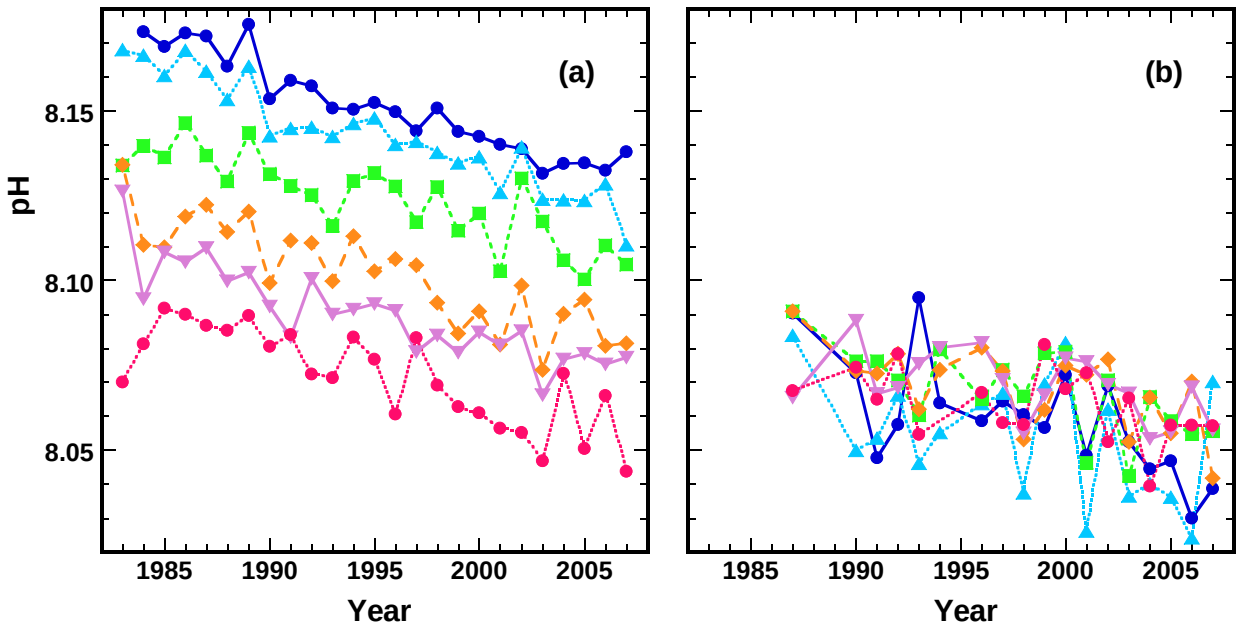

Fig. 6

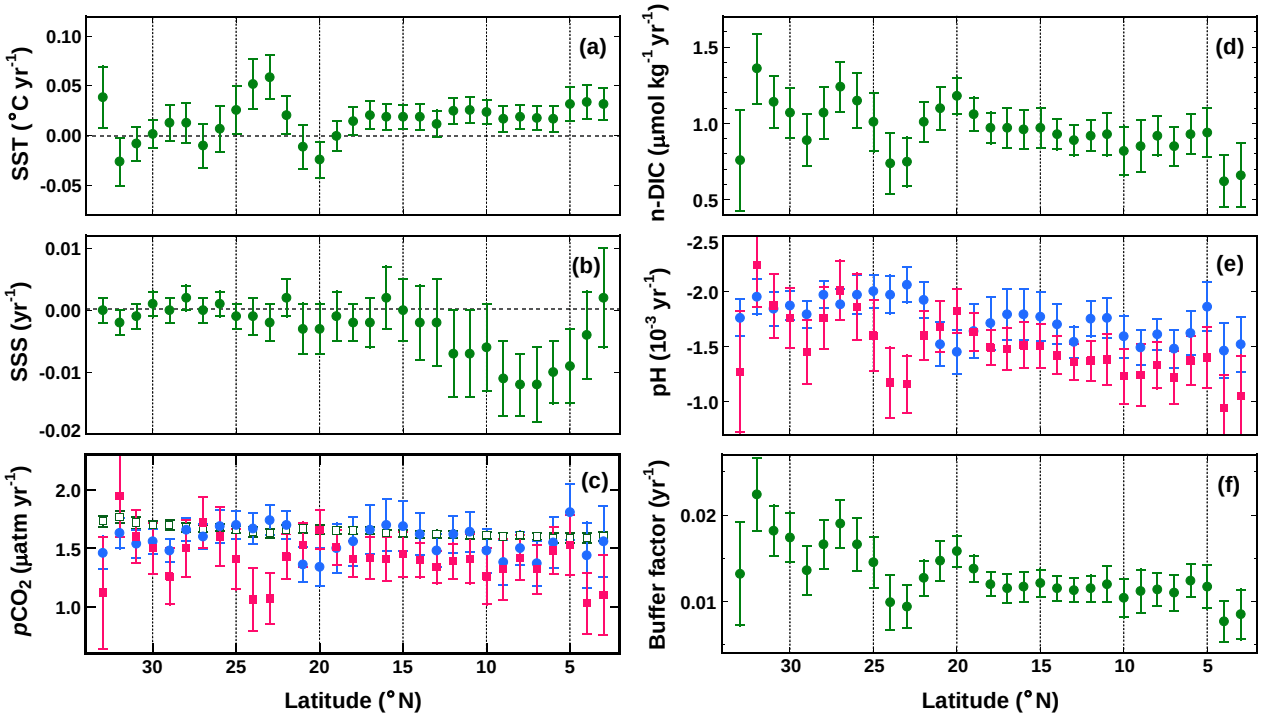
(a)
SST (°C yr-1)
0.10
0.05
0.00
-0.05
(b)
SSS (yr-1)
0.01
0.00
-0.01
-0.02
(c)
pCO2 (µatm yr-1)
2.0
1.5
1.0
30
25
20
15
10
5
Latitude (°N)
(d)
n-DIC (µmol kg-1 yr-1)
1.5
1.0
0.5
(e)
pH (10-3 yr-1)
-2.5
-2.0
-1.5
-1.0
(f)
Buffer factor (yr-1)
0.02
0.01
30
25
20
15
10
5
Latitude (°N)

Fig. 7

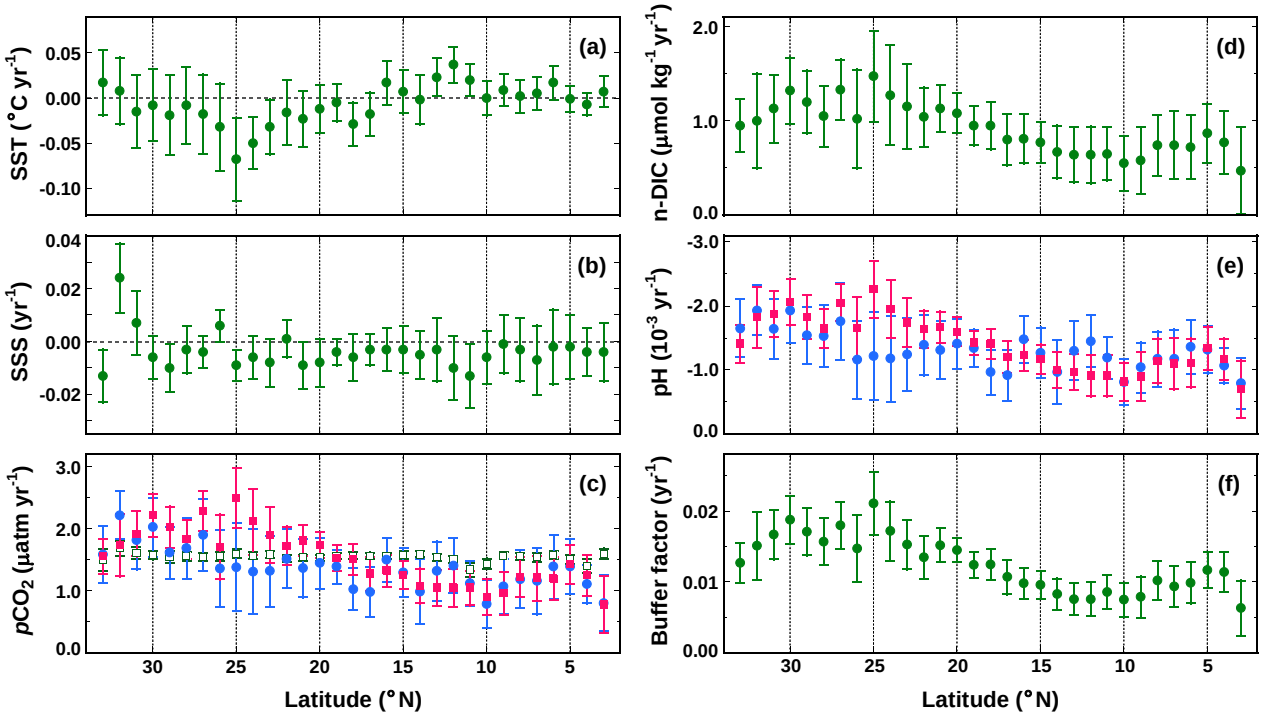
(a)
SST (°C yr-1)
0.05
0.00
-0.05
-0.10
(b)
SSS (yr-1)
0.04
0.02
0.00
-0.02
(c)
pCO2 (µatm yr-1)
3.0
2.0
1.0
0.0
30
25
20
15
10
5
Latitude (°N)
(d)
n-DIC (µmol kg-1 yr-1)
2.0
1.0
0.0
(e)
pH (10-3 yr-1)
-3.0
-2.0
-1.0
0.0
(f)
Buffer factor (yr-1)
0.02
0.01
0.00
30
25
20
15
10
5
Latitude (°N)

Fig. 8

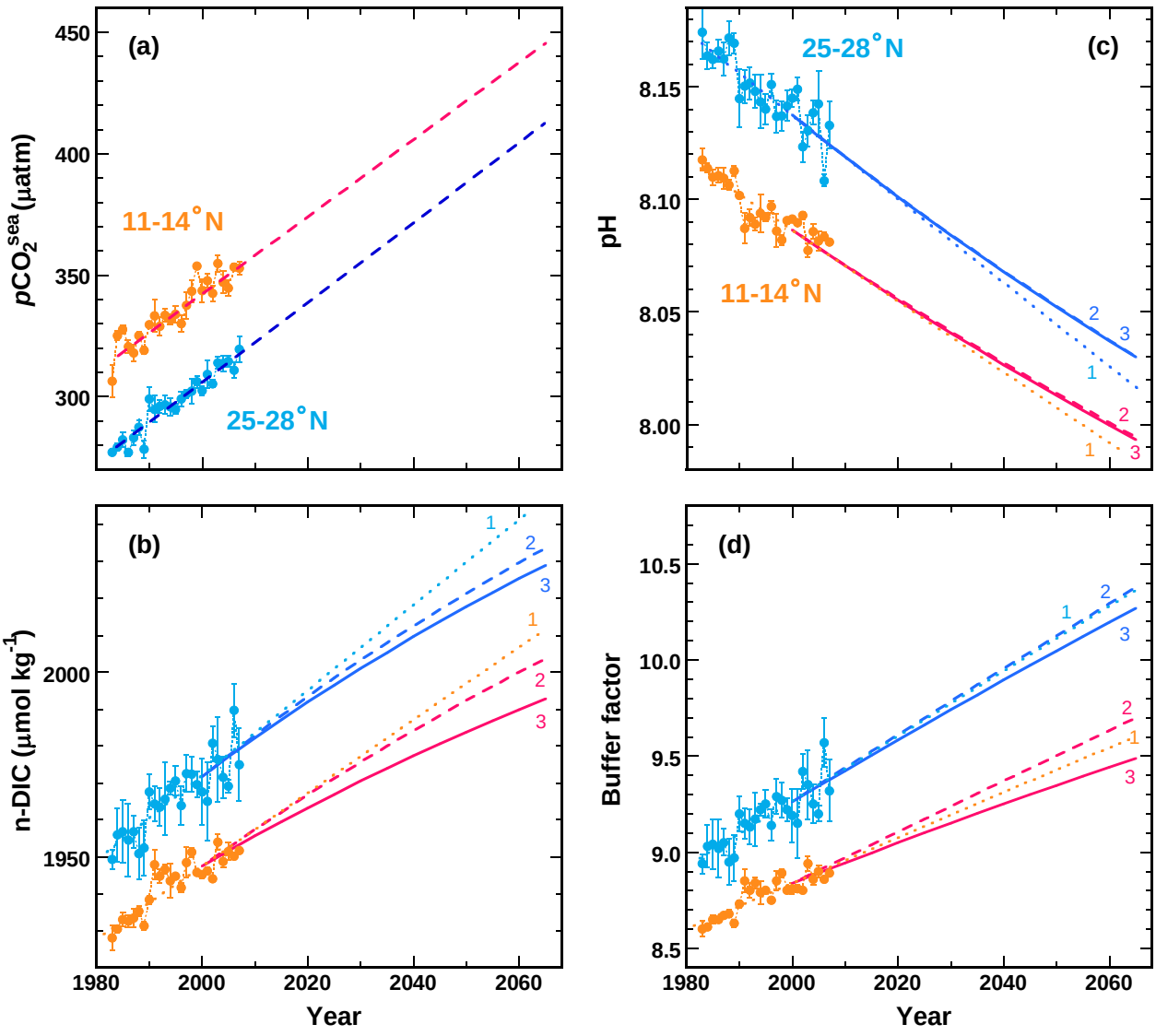
(a)
11-14°N
25-28°N
pCO_2^{sea} (µatm)
450
400
350
300
(c)
25-28°N
11-14°N
pH
8.15
8.10
8.05
8.00
1
2
3
(b)
n-DIC (µmol kg^{-1})
2000
1950
1980
2000
2020
2040
2060
Year
(d)
Buffer factor
10.5
10.0
9.5
9.0
8.5
Year

Fig. 9

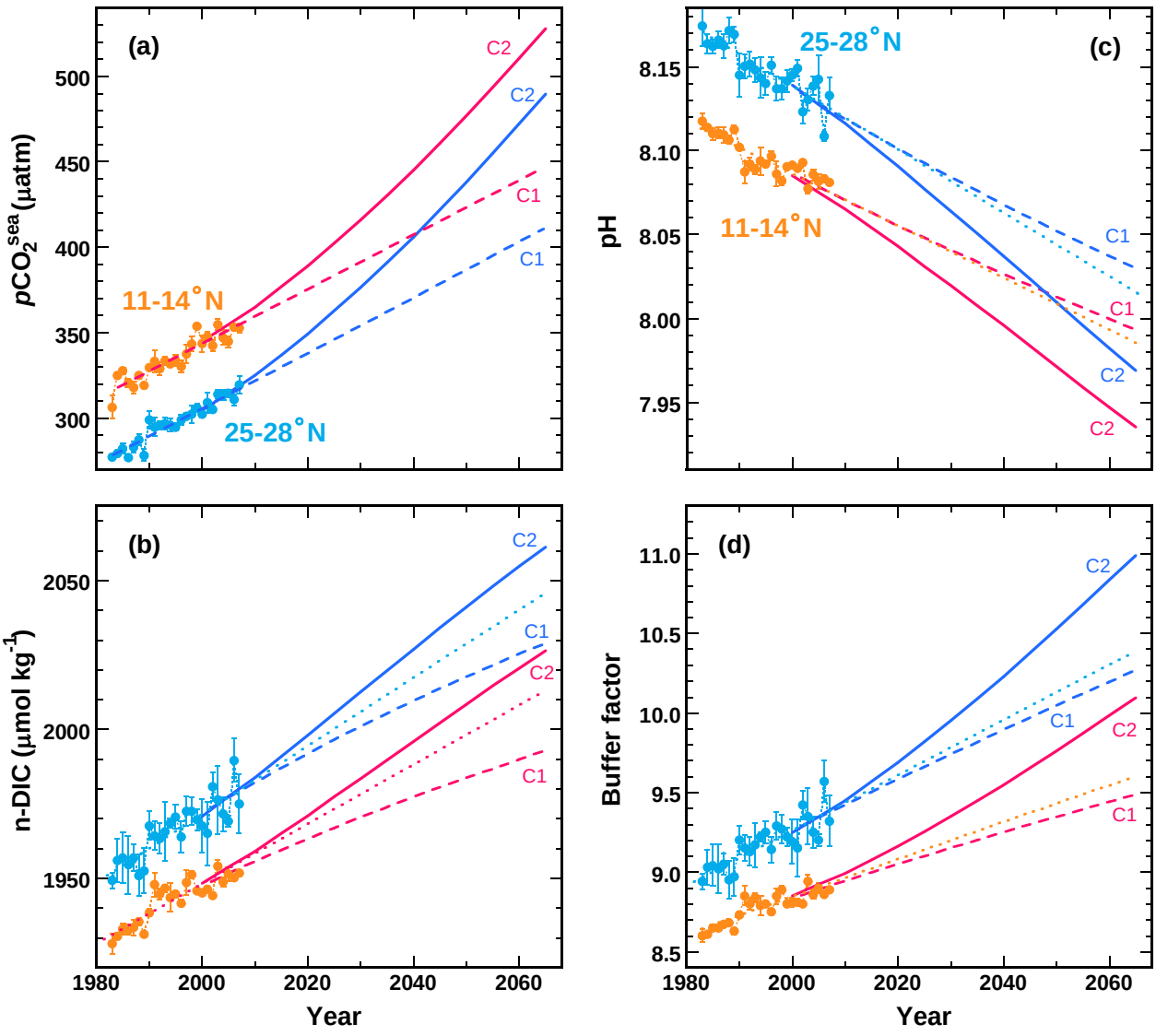
(a)
(b)
(c)
(d)
pCO_2^{sea} (µatm)
n-DIC (µmol kg^{-1})
pH
Buffer factor
Year
11-14°N
25-28°N
C1
C2
500
450
400
350
300
2050
2000
1950
8.15
8.10
8.05
8.00
7.95
11.0
10.5
10.0
9.5
9.0
8.5
1980
2000
2020
2040
2060